Articles

Spontaneous in Vitro Formation of Supramolecular β-Amyloid Structures, "βamy Balls", by β-Amyloid 1−40 Peptide†

Anita Westlind-Danielsson*,‡ and Gunnel Arnerup§

NEUROTEC, Karolinska Institute, Geriatric Medicine, Novum, KFC, S-141 86 Huddinge, Sweden, and Department of Pathology, Safety Assessment, AstraZeneca, Södertälje, Sweden

Received February 22, 2001; Revised Manuscript Received October 5, 2001

ABSTRACT: The concentration of β-amyloid peptide (Aβ), *x*−42 or *x*−40 amino acids long, increases in brain with the progression Alzheimer's disease (AD). These peptides are deposited extracellularly as highly insoluble fibrils that form densities of amyloid plaques. Aβ fibrillization is a complex polymerization process preceded by the formation of oligomeric and prefibrillar Aβ intermediates. In some of our in vitro studies, in which the kinetics of intermediate steps of fibril formation were examined, we used concentrations of synthetic Aβ that exceed what is normally employed in fibrillization studies, 300−600 μM. At these concentrations, in a cell free system and under physiological conditions, Aβ 1−40 peptide (Aβ40) forms fibrils that spontaneously assemble into clearly defined spheres, "βamy balls", with diameters of ∼20−200 μm. These supramolecular structures show weak birefringence with Congo red staining and high stability with prolonged incubation times (at least 2 weeks) at 30 °C, freezing, and dilution in H_2O. At 600 μM, they are detected after incubation for ∼20 h. Aβ peptide 1−42 (Aβ42) lacks the ability to form βamy balls but accelerates Aβ40 βamy ball formation at low stoichiometric levels (1:20 Aβ42:Aβ40 ratio). Aβ42 levels above this (=10−50% w/w) impede Aβ40 βamy ball formation. Using light (LM) and electron microscopy (EM), this study examines the gross morphology and ultrastructure of Aβ40 βamy balls and their time course of formation, in the absence and presence of Aβ42, along with some stability measures. As spheres of a misfolded protein, βamy balls resemble both AD Aβ senile plaques and neuronal inclusion bodies associated with other neurodegenerative diseases.

A number of distinct proteins have been recognized that have the propensity to lose their native secondary structure and form β-sheet-based polymeric amyloid fibrils in vivo under circumstances that are not yet well understood. Many of these misfolded proteins are recognized to be associated with human disease. At least 15 such proteins are deposited as amyloid fibrils in human tissues and are as such considered putative pathogens in a number of distinct clinical syndromes (*1*). Although the primary structure and length differ vastly for the peptides and proteins that are capable of generating these amyloid fibrils, the proteins still have several common structural denominators, placing them in a structural superfamily of their own (*2*). Given the right conditions, synthetic amyloid proteins form fibrils in vitro that are structurally indistinguishable from in situ fibrils (*1*). Synthetic fibril preparations have been used extensively as invaluable tools for examining fibril kinetics, ultrastructure, and potential in vitro neurotoxicity.

The amyloid peptide associated with Alzheimer's disease (AD),[1] Aβ, mainly *x*−42 or *x*−40 amino acids long, is deposited in the brain parenchyma forming highly insoluble amyloid plaques, aggregates of amyloid fibrils. Amyloid plaques along with neurofibrillary tangles demarcate AD pathology, setting it apart from normal brain and brains afflicted with other neurodegenerative disorders. Interest has recently focused on the polymerization steps that take the Aβ peptide from the monomer to the fibril. Studies show that the peptide forms oligomers (*3*) and larger rod-shaped structures, so-called protofibrils (*4*, *5*), which constitute intermediates of fibril formation. Cell free studies of in vitro fibrillization are usually carried out using Aβ peptide concentrations of 10−100 μM, above the critical concentration of the peptide (the minimal concentration at which

† This work has been supported by AstraZeneca, Department of Pathology, Safety Assessment, Department of Peptide Analysis, Preclinical R&D, and CNS Preclinical R&D, Södertälje, Sweden.

* To whom correspondence should be addressed: NEUROTEC, Karolinska Institute, Geriatric Medicine, KFC, Novum, Huddinge University Hospital, S-141 86 Huddinge, Sweden. Phone: +46 70 736 33 82. Fax: +46 8 585 838 80. E-mail: Anita.Westlind-Danielsson@neurotec.ki.se.

‡ Karolinska Institute.

§ AstraZeneca.

[1] Abbreviations: AD, Alzheimer's disease; Aβ, β-amyloid peptide; Aβ40, β-amyloid peptide 1−40; $Aβ40^{Gly22}$, β-amyloid peptide 1−40 with a Glu22Gly substitution; Aβ42, β-amyloid peptide 1−42; βamy ball, β-amyloid ball; βAPP, β-amyloid precursor protein; BSA, bovine serum albumin; ddH_2O, double-distilled water; CSF, cerebrospinal fluid; EM, electron microscopy; LM, light microscopy; MALDI-TOF-MS, matrix-assisted laser desorption ionization time-of-flight mass spectrometry; PBS, phosphate-buffered saline; TEM, transmission electron microscope.

10.1021/bi010375c CCC: $20.00
Published on Web 11/15/2001

polymerization is seen) (*6*). In some of our initial kinetic studies of fibrillization intermediates, we used very high Aβ40 peptide concentrations (600 μM). Surprisingly, both Aβ40 and Aβ40^{Gly22} not only formed fibrils but also self-assembled into well-defined spheres having diameters of$\sim$20−200 μm. This study describes the gross morphology, ultrastructure, formation, and stability of these spheres, which we have termed "βamy balls", and discusses what these supramolecular structures may add to the understanding of (i) amyloid formation, (ii) Aβ plaque formation, and (iii) inclusion body formation associated with other neurodegenerative diseases.

EXPERIMENTAL PROCEDURES

Materials. Aβ1−40 was purchased from Bachem (Bübendorf, Switzerland) (batch 519599) and from Biosource International/Quality Controlled Biochemicals Inc. (BI/QCB, Camarillo, CA, and Hopkinton, MA) (batches 0310621C, 0313621G, and 0313624A). Aβ1−40^{Gly22} was from BI/QCB (two separate custom-made syntheses), and Aβ1−42 was from Bachem (batches 511908 and 516817). The peptides were purchased as lyophilized trifluoroacetate salts. Bovine serum albumin (M_r = 66 000), cytochrome *c* (horse heart; M_r = 12 400), aprotinin (bovine lung; M_r = 6500), Congo red, and sodium azide (NaN_3) were from Sigma-Aldrich Fine Chemicals (St. Louis, MO). All other chemicals were of the highest available purity. The Nanosep microconcentrators (30 kDa cutoff) were from Pall Filtron Corp. (Northborough, MA). Dulbecco's modified Eagle's medium was from GibcoBRL, Life Technologies LTI (Paisley, Scotland).

Peptide Purity. According to the suppliers, all peptides were >95−99% pure on the basis of reversed phase HPLC analysis. Amino acid analysis confirmed the amino acid content and mass spectrometry the correct molecular weight. In addition, we subjected aliquots of all peptide solutions used in the βamy ball experiments to size exclusion chromatography (SEC) prior to incubation to confirm peptide quantity, identity, and purity. Samples were subjected to a wavelength scan between 200 and 400 nm using a diode-array detector (see Size Exclusion Chromatography). Peptide concentrations were determined using a standard curve in the SEC program that had been generated by correlating integrated peak absorbance units with data from quantitative amino acid analyses generated from the same samples. With the exception of Aβ40^{Gly22}, single peaks of all peptides were observed on the chromatograms immediately following dissolution in ddH_2O and 2× PBS that coincided with the known retention volumes for the monomeric, low-molecular weight (LMW) peptide species. In the case of Aβ40^{Gly22}, a small protofibrillar peak appeared in the void volume immediately upon dissolution of the lyophilized peptide as was reported previously (*7*). (The rapid protofibril formation is a hallmark of this peptide.) No other peaks representing peptide fragments, peptide with oxidized Met35, etc., could be detected with SEC under these circumstances. Occasional samples were also subjected to matrix-assisted laser desorption ionization time-of-flight mass spectrometry (MALDI-TOF-MS) and amino acid analysis (PAC, Karolinska Institute, Stockholm, Sweden). These analyses always confirmed the analytical information from the suppliers.

To further ensure that the optimum quality peptide was used, we never weighed peptide aliquots nor did we use peptide that had been frozen and thawed more than once. Instead, we dissolved the peptide in the supplier's vial directly and used all the peptide at once. Peptide concentrations were confirmed with SEC. Numerous kinetic studies in our laboratory have indicated that peptide exposure to air and water as well as extended storage at −20 °C causes peptide "aging", resulting in a low degree of experimental reproducibility.

Size Exclusion Chromatography. A Merck Hitachi D-7000 HPLC LaChrom system having a model L-7455 diode-array detector (DAD) and a model L-7100 pump was used for the chromatographic analysis. A Superdex 75 PC3.2/30 column (Amersham Pharmacia Biotech, Uppsala, Sweden) was used for the SEC separation and analysis. The column was eluted with 50 mM $Na_2HPO_4 \times NaH_2PO_4$ (pH 7.4) and 0.15 M NaCl (PBS) at a flow rate of 0.08 mL/min (pressure of 5−6 bar) at ambient temperature (22 °C). All injected samples were subjected to a wavelength scan between 200 and 400 nm. Data were extracted from measurements at 214 and 280 nm. Peak areas were integrated using Merck Hitachi model D-7000 Chromatography Data Station Software.

Incubation. A number of parameters, including temperature, were examined when attempting to optimize conditions for kinetic studies of Aβ40 fibrillization (measured as the decline in the level of LMW Aβ40) using SEC. Three different incubation temperatures were tested: 22, 30, and 37 °C. The rate of disappearance of the LMW peptide, in PBS (pH 7.4), increased significantly with temperature. Aβ β-sheet formation (*8*), fibril elongation (*9*), and aggregation (*10*) are reportedly temperature-dependent. Moreover, when long (>8 days) incubation times were employed at 30 °C, an additional SEC peak appeared in the supernatant displaying a larger retention volume than the LMW peak, suggesting peptide fragmentation. Increasing the temperature to 37 °C significantly enhanced the fragmentation rate, and that is why we decided to employ 30 °C not only for kinetic studies but also for βamy ball experiments. Self-fragmentation of Aβ40 in a water solution at 37 °C has been observed previously (*11*).

For βamy ball experiments, peptides were dissolved in double-distilled water (ddH_2O). An equal volume of 2× PBS was added giving a final PBS concentration of 50 mM $Na_2HPO_4 \times NaH_2PO_4$ (pH 7.4) and 0.1 M NaCl (±0.02% w/v NaN_3) and a final peptide concentration of 60−600 μM. Samples (150 μL) were incubated in Nanosep ultrafiltration vials at 30 °C without agitation, in the dark, for various periods of time. Incubation was discontinued by centrifuging samples in a fixed angle rotor in an Eppendorf 5417R centrifuge at 14900*g* for 10 min at 16 °C. In some experiments, such as the time course study, the centrifugation step was omitted. Eppendorf tubes were used in some experiments instead of the Nanosep vials. βamy balls formed in these vials as well, excluding the possibility that plausible impurities associated with the ultrafiltration vial were involved in βamy ball formation.

In total, six separate 8−13 day incubations were carried out when Aβ40 βamy ball formation was being investigated. In four of these incubations, Aβ40^{Gly22} samples were run in parallel, and in three experiments, samples of the Aβ40/Aβ40^{Gly22} mixture and Aβ42 were included. Light microscopic and transmission electron microscopic (TEM) examination was performed on preparations from four experiments.

Light and Electron Microscopy. When incubations had been terminated by centrifugation, βamy balls were fixed by adding 3% glutaraldehyde to the ultrafiltration chamber holding the filter with the pelleted βamy balls. Samples with glutaraldehyde were then centrifuged again at the same centrifugation settings. The tube was then refilled with glutaraldehyde and refrigerated until fixation and staining procedures were continued. Filters were then removed from the Nanosep tube and postfixed in OsO_4 (2%). Epoxy plastic embedding of the filters was preceded by dehydration. For LM examination, semithin (1 μm) sections were cut and stained with toluidine blue. Ultrathin (70−80 nm) sections were prepared for EM examination using uranyl acetate and lead citrate as stains. A Philips CM10 transmission electron microscope was used for the EM studies. Preparations were examined and photographed under several different EM magnifications, including 11.5K×, 28.5K×, 52K×, and 105K×. For the time course study and some additional studies, aliquots were taken directly from the incubation vials, omitting the centrifugation step, and were then stained with toluidine blue before being examined with LM. Samples were prepared for Congo red staining by first drying them on a heating plate, washing them with ddH_2O, and then drying them again before staining them according to standard procedures.

In the preparation for the negative stain, 8 μL samples were applied to a grid covered by a carbon-stabilized Formvar film (Ted Pella, Inc., Redding, CA). Excess fluid was removed with a filter paper after 1 min, after which 8 μL of 1% uranyl acetate (E. Merck, Darmstadt, Germany) was applied to the sample. Excess fluid was removed with a filter paper after 1 min.

RESULTS

In initial experiments, Aβ40 peptides [Aβ40, Aβ40^{Gly22}, or a mixture of the two (1:2 or 4:5 Aβ40:Aβ40^{Gly22} ratio)], incubated for 8 days, were found to spontaneously assemble into supramolecular spherical structures from 600 μM peptide solutions. These structures, termed β-amyloid balls or βamy balls, were found to have diameters of 20−200 μm, most commonly 50−100 μm (Figure 1). The volume of a typical βamy ball (100 μm) is thus 0.52 nL. βamy ball formation was also evident when Aβ40 levels were reduced to 300 μM. They can be seen with LM with or without fixation and/or staining at a magnification of 9×. βamy balls pelleted by centrifugation on the Nanosep filter have a gelatinous consistency. When this preparation is fixed and stained and examined with LM, βamy balls exhibit some distinct gross morphological features that are dependent on what peptide is used for their generation. For example, those βamy balls generated from Aβ40 lack a central core density and are after long incubation times found to be surrounded by a halo (Figure 1a). In contrast, a central core density is apparent in Aβ40^{Gly22} (Figure 1b) and Aβ40^{Gly22}/Aβ40 (Figure 1c) βamy balls. In addition, Aβ40^{Gly22} βamy balls form large "honeycomb" formations on the Nanosep ultrafiltration membrane (Figure 1c). This has not been observed for Aβ40. Aβ40^{Gly22} βamy balls seem more prone to adhere to one another than Aβ40 βamy balls, which may be a reflection of the higher hydrophobicity that Aβ40^{Gly22} displays. The centrifugation-induced packing of the Aβ40^{Gly22} βamy balls on the membrane causes compression, giving the LM impression of "cells" having a "double-layer membrane" (not a halo) and a "nucleus-like" central density (Figure 1c). Also, the βamy balls closest to the Nanosep membrane have lost their round form during centrifugation (Figure 1c).

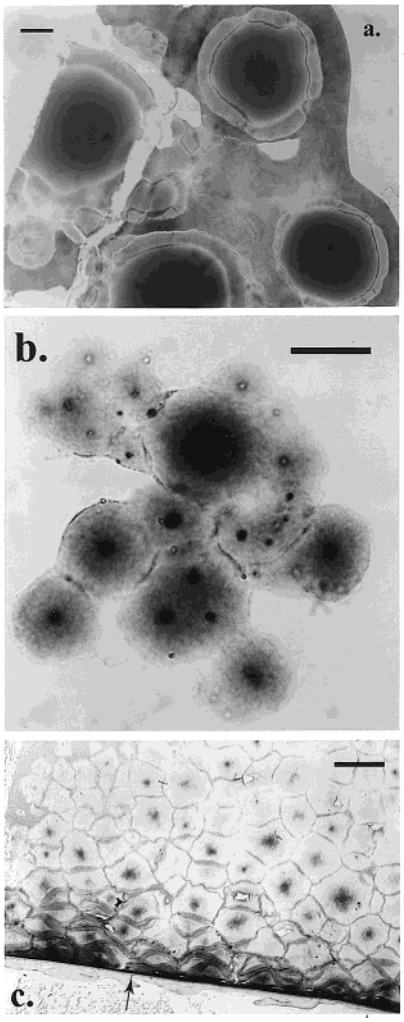

FIGURE 1: Gross morphology of βamy balls composed of Aβ40 (a), Aβ40 and Aβ40^{Gly22} (1:2) (b), and Aβ40^{Gly22} (c). Semithin section of epoxy-embedded βamy balls showing four βamy balls with diameters of ∼100 μm having a homogeneous core and a distinct halo, formed from a 600 μM peptide solution after an incubation period of 8 days (scale bar = 30 μm) (a). Clusters of glutaraldehyde-fixed βamy balls with variable diameters, a distinct "nucleus", and no halo in a drop of incubation fluid formed after an incubation period of 5 days as seen under the light microscope (bar = 50 μm) (b). A vertical 1 μm thick section of an epoxy-embedded honeycomb formation on a Nanosep membrane after an incubation period of 8 days. The arrow denotes the boundary between the βamy balls and the filter. Many of these βamy balls are >100 μm in diameter. βamy balls close to the filter surface have been compressed during the centrifugation step (bar = 150 μm) (c).

Electron micrographs of ultrathin sections of βamy balls show that these are made up of fibrils. This is shown in Figure 2a (Aβ40) and Figure 2b (Aβ40^{Gly22}) and applies to a mixture of the two peptides as well (1:2 or 4:5; not shown). The fibrils fulfill the morphological criteria of Aβ fibrils in that they have a diameter of ∼6−10 nm and they show birefringence under polarized light when stained with Congo red, although this birefringence is difficult to obtain. The fibrils are oriented in all directions, and it is easy to

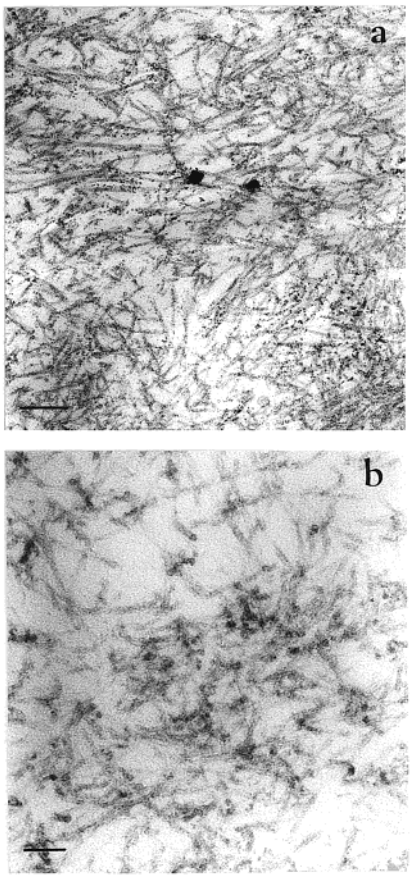

FIGURE 2: Typical electron micrographs of βamy ball sections. Aβ40 fibrils (bar = 50 nm) (a). Higher magnification of Aβ40^{Gly22} βamy ball fibrils (bar = 20 nm) (b).

distinguish individual fibrils. Fibrils also make up the halo of Aβ40 βamy balls. The halo shows higher fibril density than the βamy ball cores, and the halo fibrils are more prone to a parallel orientation (not shown).

The high peptide concentrations that were employed here prompted us to investigate whether some proteins, not known to form amyloid, formed fibrils and/or spheres under these conditions as well. Three different globular proteins, bovine serum albumin, cytochrome *c*, and aprotinin, were subjected to the experimental protocol for generating βamy balls. LM examination did not reveal any sphere formation, nor did the EM pictures presented in Figure 3b−d reveal any fibrillization tendency.

In contrast to the globular proteins examined above, Aβ42 is highly amyloidogenic and is even more inclined to form amyloid fibrils than Aβ40. Despite this, Aβ42, at 600 μM, instantly formed fibril bundles ~200 nm to 1 μm thick (Figure 4) that in turn assemble into large nets, and not βamy balls (Figure 5). Curiously, these nets tend to arrange into extraordinary, large (>200 μm), cagelike structures where the netlike appearance is derived from fibril bundle structures that resemble "planar" polygons in the light microscope (Figure 5b). The nets and netlike cages, in turn, tend to aggregate. Similar results were found with lower concentrations of Aβ42 (60 and 120 μM).

Aβ42 fibril bundles show intense birefringence in plane-polarized light after Congo red staining (not shown). Negative stains of the bundles more clearly reveal their fibrillar nature (Figure 4b) than do the stained sections (Figure 4a). The same types of netlike structures were seen when Aβ42 was mixed with Aβ40 (see below), but only when the percentage Aβ42 equaled or exceeded 20%. Interestingly, fixed Aβ40 βamy balls realized a similar, but not as ordered, netlike appearance when they were left to dry in air (not shown).

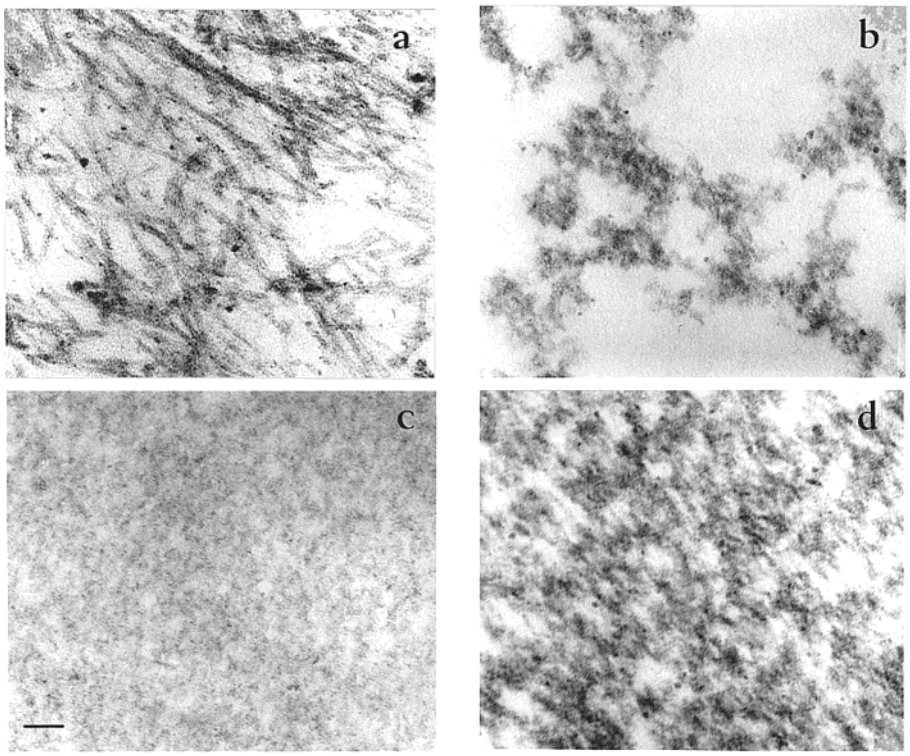

FIGURE 3: Aβ40 and three globular, nonamyloidogenic, proteins viewed with a high-magnification TEM: Aβ40 (a), aprotinin (b), BSA (c), and cytochrome *c* (d) (bar = 20 nm).

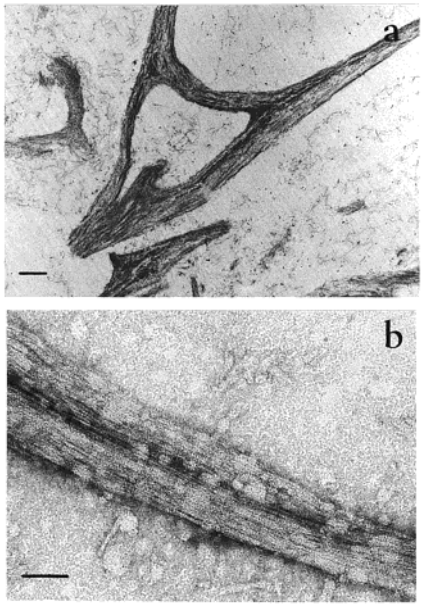

FIGURE 4: Electron micrographs of Aβ42 fibril bundles visualized using two different EM preparation protocols. Ultrathin section of fibril bundle formation (bar = 250 nm) (a) and a fibril bundle visualized using negative stain (bar = 100 nm) (b).

Table 1: Abundance of Aβ40 and Aβ40/Aβ42 βamy Balls in PBS after Various Incubation Times[a]

Aβ peptide	20 h	3−4 days	1−2 weeks
Aβ40	+	++	++++
Aβ42	−	−	−
Aβ40 and Aβ42 (5%)	+++	+++++	+++++
Aβ40 and Aβ42 (10%)	−	++	+++
Aβ40 and Aβ42 (20%)	−	−	+
Aβ40 and Aβ42 (50%)	−	−	−

[a] The total peptide concentration in each Nanosep incubation vial was 600 μM. Observations were carried out on 3 × 5 μL of a toluidine-stained aliquot incubation solution using LM. Data are the result of two separate experiments.

A time course study was conducted where peptides were incubated anywhere from 2 h to 11 days. LM and toluidine staining were used for βamy ball detection. βamy ball formation from 600 μM Aβ40 was compared to that from Aβ40 mixed with various percentages of Aβ42 to give a final total peptide concentration of 600 μM (Table 1). It takes at least 20 h for Aβ40 βamy balls to form under the given conditions. When the peptide composition is changed to 95% Aβ40 and 5% Aβ42, βamy balls become visible within 6 h and are abundant at 24 h. Counting the number of βamy balls in three LM visual fields from 3 × 5 μL incubation fluid samples after a 24 h incubation period showed that the number of Aβ40 βamy balls was 69 ± 10 (mean ± the standard error of the mean), while it was >500 in the 95% Aβ40/5% Aβ42 mixture. Substituting 10 or 20% Aβ40 for Aβ42 did not enhance βamy ball formation further, but in contrast impeded formation. Thus, the more Aβ42 that was added (=10%), the stronger the inhibiting effect. No βamy balls were detected for up 11 days (Table 1) when Aβ42 constituted half of the amount of peptide in an Aβ40/Aβ42 mixture.

Time course studies of βamy ball formation, using 300 and 600 μM Aβ, introduced a conception of how βamy balls could be formed (Figure 6a−d). Prior to βamy ball formation, clouds of toluidine-stained peptide can be distinguished. Small densities of peptide eventually begin to take form (Figure 6a). The densities grow and attain a "cotton ball"-like appearance with a fuzzy periphery (Figure 6b). When ambient peptide levels decline significantly, the cotton ball forms a distinct peripheral boundary (Figure 6c). Peptide attracted to this sphere at a later stage in time will form the halo (Figure 6d and Figure 1a). As mentioned earlier, we have not seen any halo surrounding βamy balls of Aβ40^{Gly22} or mixtures of Aβ40^{Gly22} and Aβ40. This could indicate that the Aβ40^{Gly22} interpeptide attraction is so strong and thereby rapid that little peptide escapes the developmental phase from cloud to cotton ball having a clearly defined periphery. Our previous studies of Aβ40^{Gly22} protofibril formation support this contention (*7*).

The experiments described above where long incubation times were employed were also carried out in the presence of NaN_3 (0.02%) to inhibit bacterial growth. LM or EM could not reveal any difference in the βamy ball morphology with or without NaN_3 present (not shown). Finally, βamy balls are strikingly stable at 30 °C in a water solution. They do not seem to change their shape or morphology for at least 2 weeks in PBS, nor are they visibly affected by dilution (1:2) in cell culture media. They withstand refrigeration for up to 3 days after 1:10 dilution in H_2O, freezing (−70 °C), and thawing.

DISCUSSION

This work describes conditions that support the spontaneous assembly of Aβ40 and Aβ40^{Gly22} into fibril-packed spheres that we call βamy balls, and gives an account of their structural nature. These in vitro formations have, to our knowledge, not been reported earlier and constitute a striking

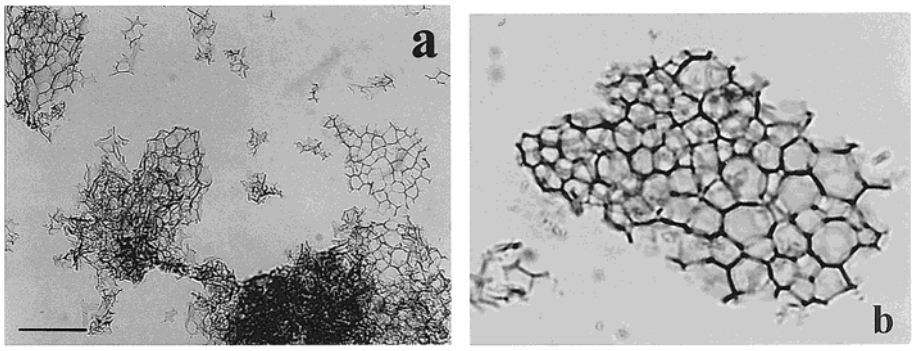

FIGURE 5: LM image of supramolecular structures of Aβ42 fibril bundles. Cage- and netlike formations of Aβ42 (600 μM) in buffer after incubation for 14 days (scale bar = 50 μm) (a). A detail of a netlike cage of Aβ42 fibrils at slightly higher magnification (b).

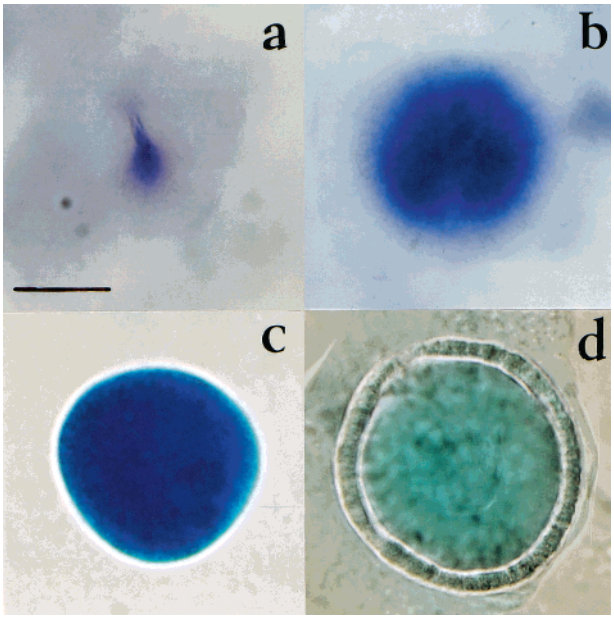

FIGURE 6: Photographs of LM views of plausible sequential events leading to the formation of Aβ40 βamy balls with an incubation period of 5 days. All four pictures are taken using the same magnification, but not of the same βamy ball or "pre"-βamy ball formation. An initial peptide density forms, a possible starting point that attracts more peptide (a) that generates a sphere giving a fuzzy cotton ball image (b). When the surrounding peptide levels fall (here seen by the disappearance of toluidine blue in the surrounding solution), the peripheral boundary becomes sharper and the volume becomes set by the formation of a distinct periphery (c). Additional material drawn to the sphere forms a halo around the periphery (d). The peptide concentration was 600 μM (scale bar = 35 μm, which pertains to panels a−d).

example in which chemical properties of proteins by far exceed the sum of the properties of their constituent amino acids. βamy ball formation imparts an additional dimension to amyloid formation and is a fascinating example of protein self-assembly at the supramolecular level. The results of the study also emphasize that the nature of fibril−fibril interactions is strongly dependent on the peptide or protein makeup of the fibrils. Moreover, fibrils of various compositions may form suprafibrillar structures that will exhibit structural differences at the supramolecular level that will show vastly different fibril surface areas exposed to the surroundings. Both qualitative (*12*) and quantitative aspects of fibril surface are critical determinants of the purported neurotoxic nature of amyloid fibrils.

Concentrations of Aβ used in this study by far exceed levels of Aβ detected in human cerebrospinal fluid (CSF) (*13*) and plasma (*14*). CSF and plasma levels of Aβ are not likely to justly reflect pathologically high Aβ levels that are certain to prevail in the milieu surrounding the amyloid plaques of the diseased Alzheimer brain. With the progression of the disease, these regions will most likely reach very high Aβ concentrations. Apart from the increased peptide concentration, a number of factors are capable of shifting the Aβ polymerization reaction, monomer → fibril, to the right, including increased incubation time, augmented temperature, enhanced ionic strength, pH at or close to the isoelectric point, agitation, structural alterations of Aβ, including N-terminal truncations, and the presence of ancillary compounds or interactive surfaces. These factors may have a strong impact on the fate of the peptide in local extracellular microenvironments even though Aβ concentrations may not even reach the critical concentration in the AD brain. However, increasing Aβ peptide concentrations can be thought of as a substitute for these factors when experimentally elaborating on pure peptide solutions.

Why βamy balls have escaped detection until now in in vitro experimental systems may be related to the high peptide concentration required for their generation. Conditions that make in vitro experimentation practicable include the use of lower Aβ concentrations and contracted time frames. However, in light of the discussion above concerning factors affecting fibrillization rate, addition of Aβ40 to a complex experimental system such as cell culture, at concentrations below those used here, may well lead to βamy ball formation. Here they are certain to be difficult to discover. Possibly, undetected βamy ball formation may offer one explanation for why Aβ40 neurotoxicity studies in cell culture are often associated with difficulties in obtaining reproducible results. Furthermore, βamy ball formation may easily escape detection in in vitro fibrillization studies due to the way Aβ samples are handled prior to examining fibrils (e.g., sonication and negative stain).

Aβ40^{Gly22} is one of the proteolytic products of the β-amyloid precursor protein (βAPP) derived from a mutation in the Aβ coding region of the βAPP gene. This "Arctic" mutation was recently described in a Swedish family where it is associated with typical clinical symptoms of AD (*7*). This single-amino acid substitution at position 22 (Glu → Gly) expresses itself as enhanced kinetics and thermodynamic characteristics of Aβ40^{Gly22} protofibrils compared to Aβ40 protofibrils. Both the rate and magnitude of protofibril formation increase (*7*), the disaggregation rate is attenuated and β-sheet formation accelerated (unpublished experiments). Nevertheless, Aβ40^{Gly22} still has the ability to form βamy balls, contrasting sharply with the thick fibril bundles formed by Aβ42. Thus, although the Gly22 substitution renders Aβ40^{Gly22} more hydrophobic, its fibril surface characteristics, such as charge and hydrophobicity, resemble those of Aβ40 more than those of Aβ42.

Aβ42 does not form βamy balls but rapidly produces bundles of fibrils that form big netlike cages that in turn cluster into larger aggregates. These aggregates resemble the amorphous zones of Aβx−42/43 fibril bundles that make up AD diffuse plaques that lack distinct boundaries. The diffuse plaques are primarily composed of Aβx−42/43 in AD (*15*), Down's syndrome (*16*), FAD (*17*), and nondemented aged (*18*), and are predicted to be an initial stage in plaque formation. Together with immature (uncored) and mature (cored) plaques, these represent three categories of plaques found in AD brains (*19*). They all primarily contain Aβx−42/43 in AD and Down's syndrome (*15*) and in FAD (*15*, *20*).

In contrast to the thick, compacted Aβ42 fibril bundles, one is struck by the fact that fibril density is much lower in the Aβ40 βamy balls where single Aβ40 fibrils can easily be distinguished in EM sections. It is possible that the reduced fibril density could explain why it is more difficult to detect red/green birefringence for βamy balls than for Aβ42 fibril bundles. The differences again suggest that Aβ40 and Aβ42 fibril surfaces have distinct chemical characteristics. The hydrophobic amino acids Ile41 and Ala42 that extend Aβ40 C-terminally are the candidates effecting this

difference, known to be critical to amyloid nucleation (*21*), fibril structure, and solubility (*22*).

The time course studies, where the Aβ42:Aβ40 molar ratio is varied, show that (a) at a 1:20 ratio βamy ball formation is significantly augmented, compared to that with Aβ40 alone, whereas (b) lower ratios, 1:10 and 1:5, prolong βamy ball formation. The higher the Aβ42 concentration, the longer the lag phase preceding the appearance of βamy balls at molar ratios of $\geq$1:5. Although 300 μM Aβ40 is a sufficiently high concentration to support βamy ball formation, a 300 μM Aβ40/300 μM Aβ42 mixture (1:1) does not. Amyloid fibrillization of a single peptide species has been proposed to occur in a nucleation-dependent manner (*23*) followed by a rapid fibril extension phase (*24*). Nucleation is thermodynamically unfavorable and is therefore the rate-limiting step. Aβ42 is both more prone to nucleate and fibrillize than Aβ40 (*5*). However, Aβ40 and Aβ42 coexist in the brain, giving potential room for distinct in vivo fibrillization kinetics other than those described for either peptide alone in vitro. In recent studies using fluorescence spectroscopy and thioflavin T, the kinetics of Aβ40 and Aβ42 interaction were examined. Aβ40 and Aβ42 were found to exert mutual inhibition on fibrillization, suggested to occur as a result of conformational constraints that arise during the nucleation phase (*25*). These results agree well with our findings mentioned in part b above. In part a, however, we used levels of Aβ42 (5%) lower than those used by Hasegawa et al. (*25*). The resulting augmentation in the rate of βamy ball formation at the lowest Aβ42:Aβ40 (1:20) ratio is puzzling. A possible explanation for the phenomenon is that Aβ42 nuclei (or seeds) form rapidly and in large quantities under these conditions (20 μM Aβ42), enabling effective seeding of Aβ40 (*5*, *25*). At very low levels, Aβ42 may still initiate an Aβ40 conformational transition without interfering with the Aβ40 elongation phase. On the other hand, if sufficiently high concentrations of Aβ42 are present, Aβ42 may compete with and possibly even block the Aβ40 fibril elongation phase, under the assumption that Aβ42 has a much higher affinity for Aβ42 nuclei than Aβ40.

Aβ40 levels are reportedly higher than those of Aβ42 in medium conditioned by cultured cells (*26*−*28*), in human CSF (*13*), and in human plasma (*14*). The opposite has been reported for AD brain (*29*, *30*) and plaques (*15*, *18*). FAD mutations almost invariably lead to elevated Aβ42 levels in plasma (*14*) and in plaques (*15*, *20*). From these and many other studies, a consensus has evolved that the majority of plaques are initially formed and composed of Aβx−42/43. The central role in plaque formation and composition has given Aβ42 a stronghold on the candidacy of being the main driving force in disease initiation and progression, and as mentioned earlier, Aβ42 has the ability to act as a seed, as a consequence initiating and catalyzing Aβ fibrillization (*31*). However, by extrapolation of the consequences of the time course studies by Hasegawa et al. (*25*) and by us to brain, with its prevailing high Aβ42:Aβ40 ratios, it is possible that Aβ42 may effectively hinder Aβ40 fibril formation in vivo. The low level of Aβ40 in plaques (*15*, *18*), in particular early in the disease, supports this contention. Interestingly, there is a trend toward a decline in the Aβ42:Aβ40 ratio in several cortical brain regions with disease progression measured as a function of the level of deterioration of cognitive abilities (*29*). Although Aβ40 seems to have a less dominating role in brain than Aβ42 on a quantitative and plaque-forming basis, its conceivable role in AD is still unknown. On this note, it is interesting to recognize the findings pertaining to the microglial preference for Aβ40-containing plaques. The majority of Aβ40 positive plaques are mature plaques, and the observations include plaque-associated microglia in AD (*32*, *33*) and nondemented aged individuals (*32*) as well as in individuals with Down's syndrome (*33*). βamy balls may be one commendable model system for testing hypotheses associated with the Aβ40−microglia relationship.

The longevity that neurons display is more likely associated with morphological alterations during aging than noted for other cell types. Besides plaques and neurofibrillary tangles in AD, various morphological changes are conspicuous in a number of neurodegenerative diseases, including Lewy body (*34*) and polyglutamine diseases (*35*), and in transmissible spongiform encephalopathies (*36*). βamy balls resemble several spherical protein inclusion bodies associated with these diseases, including Lewy bodies (*37*), polyglutamine inclusion bodies (*38*), Kuru, Gertsmann-Straüssler-Scheinker, and Creutzfeld-Jacob plaques (*39*), and also Pick's bodies (*34*), with respect to size, shape, and the misfolded protein fibrillar nature of their content. For instance, at the LM level, Aβ40 βamy balls surrounded by a peripheral halo are strikingly similar to the Lewy bodies found in the substantia nigra pars compacta of the Parkinson brain (*37*), which are also surrounded by a halo. The assembly of Aβ into fibril-packed spheres drastically reduces the level of Aβ exposure to the surroundings. It is tempting to speculate, along with the ideas voiced in the early days of amyloid research, that amyloid plaque formation represents a means of ridding the cell of potential pathogens, radically diminishing their level of exposure to the surroundings. Neurotoxicity studies with βamy balls should shed light on this issue.

Aβ plaques are complex biochemical entities, and their evolution, maturation in human brain, and role in disease still remain obscure. Besides neuronal and glial cellular elements, they have been found to be associated with a long line of ancillary components, including glycosaminoglycans (GAGs) such as heparan sulfate proteoglycan (*39*), Apo J (*40*), amyloid P component (*41*), Apo E (*42*), complement factors (*43*), albumin (*44*), α1-antichymotrypsin (*45*), α2-macroglobulin (*46*), and α-synuclein (*47*). The experimental use of βamy balls may help tease out the potential roles of amyloid-associated components (i) in catalyzing amyloid fibril formation, (ii) as conceivable neurotoxic elements, or (iii) as modulators of fibril morphology, stability, or solubility. Moreover, it will be interesting to determine whether βamy ball-like structures may emanate from the major protein components of any of the inclusion bodies mentioned above under similar in vitro incubation parameters as used here, or from other amyloid proteins.

ACKNOWLEDGMENT

We gratefully acknowledge Drs. Anders Undén, Erik Danielsson, and Marianne Schultzberg for their valuable comments on the manuscript.

REFERENCES

1. Kisilevsky, R., and Fraser, P. E. (1997) *Crit. Rev. Biochem. Mol. Biol. 32*, 361−404.

2. Sunde, M., Serpell, L. C., Bartlam, M., Fraser, P. E., Pepys, M. B., and Blake, C. C. (1997) *J. Mol. Biol. 273*, 729−739.
3. Lambert, M. P., Barlow, A. K., Chromy, B. A., Edwards, C., Freed, R., Liosatos, M., Morgan, T. E., Rozovsky, I., Trommer, B., Viola, K. L., Wals, P., Zhang, C., Finch, C. E., Krafft, G. A., and Klein, W. L. (1998) *Proc. Natl. Acad. Sci. U.S.A. 95*, 6448−6453.
4. Harper, J. D., Wong, S. S., Lieber, C. M., and Lansbury, P. T. (1997) *Chem. Biol. 4*, 119−125.
5. Walsh, D. M., Lomakin, A., Benedek, G. B., Condron, M. M., and Teplow, D. B. (1997) *J. Biol. Chem. 272*, 22364−22372.
6. Harper, J. D., and Lansbury, P. T., Jr. (1997) *Annu. Rev. Biochem. 66*, 385−407.
7. Nilsberth, C., Westlind-Danielsson, A., Eckman, C. B., Condron, M. M., Axelman, K., Forsell, C., Stenh, C., Luthman, J., Teplow, D. B., Younkin, S. G., Naslund, J., and Lannfelt, L (2001) *Nat. Neurosci. 4*, 887−893.
8. Gursky, O., and Aleshkov, S. (2000) *Biochim. Biophys. Acta 1476*, 93−102.
9. Kusumoto, Y., Lomakin, A., Teplow, D. B., and Benedek, G. B. (1998) *Proc. Natl. Acad. Sci. U.S.A. 95*, 12277−12282.
10. Snyder, S. W., Ladror, U. S., Wade, W. S., Wang, G. T., Barrett, L. W., Matayoshi, E. D., Huffaker, H. J., Krafft, G. A., and Holzman, T. F. (1994) *Biophys. J. 67*, 1216−1228.
11. Hensley, K., Carney, J. M., Mattson, M. P., Aksenova, M., Harris, M., Wu, J. F., Floyd, R. A., and Butterfield, D. A. (1994) *Proc. Natl. Acad. Sci. U.S.A. 91*, 3270−3274.
12. Fezoui, Y., Hartley, D. M., Walsh, D. M., Selkoe, D. J., Osterhout, J. J., and Teplow, D. B. (2000) *Nat. Struct. Biol. 7*, 1095−1099.
13. Vigo-Pelfrey, C., Lee, D., Keim, P., Lieberburg, I., and Schenk, D. B. (1993) *J. Neurochem. 61*, 1965−1968.
14. Scheuner, D., Eckman, C., Jensen, M., Song, X., Citron, M., Suzuki, N., Bird, T. D., Hardy, J., Hutton, M., Kukull, W., Larson, E., Levy-Lahad, E., Viitanen, M., Peskind, E., Poorkaj, P., Schellenberg, G., Tanzi, R., Wasco, W., Lannfelt, L., Selkoe, D., and Younkin, S. (1996) *Nat. Med. 2*, 864−870.
15. Iwatsubo, T., Odaka, A., Suzuki, N., Mizusawa, H., Nukina, N., and Ihara, Y. (1994) *Neuron 13*, 45−53.
16. Mann, D. M., and Iwatsubo, T. (1996) *Neurodegeneration 5*, 115−120.
17. Mann, D. M., Iwatsubo, T., Ihara, Y., Cairns, N. J., Lantos, P. L., Bogdanovic, N., Lannfelt, L., Winblad, B., Maat-Schieman, M. L., and Rossor, M. N. (1996) *Am. J. Pathol. 148*, 1257−1266.
18. Fukumoto, H., Asami-Odaka, A., Suzuki, N., Shimada, H., Ihara, Y., and Iwatsubo, T. (1996) *Am. J. Pathol. 148*, 259−265.
19. Masliah, E., Terry, R. D., Mallory, M., Alford, M., and Hansen, L. A. (1990) *Am. J. Pathol. 137*, 1293−1297.
20. Lemere, C. A., Lopera, F., Kosik, K. S., Lendon, C. L., Ossa, J., Saido, T. C., Yamaguchi, H., Ruiz, A., Martinez, A., Madrigal, L., Hincapie, L., Arango, J. C., Anthony, D. C., Koo, E. H., Goate, A. M., Selkoe, D. J., and Arango, J. C. (1996) *Nat. Med. 2*, 1146−1150.
21. Jarrett, J. T., Berger, E. P., and Lansbury, P. T., Jr. (1993) *Biochemistry 32*, 4693−4697.
22. Jarrett, J. T., Costa, P. R., Griffin, R. G., and Lansbury, P. T., Jr. (1994) *J. Am. Chem. Soc. 116*, 9741−9742.
23. Jarrett, J. T., and Lansbury, P. T., Jr. (1993) *Cell 73*, 1055−1058.
24. Naiki, H., and Nakakuki, K. (1996) *Lab. Invest. 74*, 374−383.
25. Hasegawa, K., Yamaguchi, I., Omata, S., Gejyo, F., and Naiki, H. (1999) *Biochemistry 38*, 15514−15521.
26. Dovey, H. F., Suomensaari-Chrysler, S., Lieberburg, I., Sinha, S., and Keim, P. S. (1993) *NeuroReport 4*, 1039−1042.
27. Seubert, P., Vigo-Pelfrey, C., Esch, F., Lee, M., Dovey, H., Davis, D., Sinha, S., Schlossmacher, M., Whaley, J., Swindlehurst, C., McCormack, R., Wolfert, R., Selkoe, D. J., Lieberburg, I., and Schenk, D. (1992) *Nature 359*, 325−327.
28. Suzuki, N., Cheung, T. T., Cai, X. D., Odaka, A., Otvos, L., Jr., Eckman, C., Golde, T. E., and Younkin, S. G. (1994) *Science 264*, 1336−1340.
29. Naslund, J., Haroutunian, V., Mohs, R., Davis, K. L., Davies, P., Greengard, P., and Buxbaum, J. D. (2000) *J. Am. Med. Assoc. 283*, 1571−1577.
30. Roher, A. E., Loweson, J. D., Clarke, S., Wolkow, C., Wang, R., Cotter, R. J., Reardon, I. M., Zurcher-Neely, H. A., Heinrikson, R. L., Ball, M. J., and Greenberg, B. D. (1993) *J. Biol. Chem. 268*, 3072−3083.
31. Jarrett, J. T., and Lansbury, P. T., Jr. (1992) *Biochemistry 31*, 12345−12352.
32. Fukumoto, H., Asami-Odaka, A., Suzuki, N., and Iwatsubo, T. (1996) *Neurodegeneration 5*, 13−17.
33. Mann, D. M., Iwatsubo, T., Fukumoto, H., Ihara, Y., Odaka, A., and Suzuki, N. (1995) *Acta Neuropathol. 90*, 472−477.
34. Lowe, J. (1994) in *Neurodegenerative Diseases* (Calne, D. B., Ed.) pp 51−69, W. B. Saunders Co., Philadelphia.
35. Paulson, H. L. (2000) *Brain Pathol. 10*, 293−299.
36. Brown, P. (1994) in *Neurodegenerative Diseases* (Calne, D. B., Ed.) pp 839−876, W. B. Saunders Co., Philadelphia.
37. Brion, S., Plas, J., and Bereanu, A. (1991) in *The Pathology of the Aging Human Nervous System* (Duckett, S., Ed.) pp 88−93, Lea & Febiger, Philadelphia.
38. Paulson, H. L. (1999) *Am. J. Hum. Genet. 64*, 339−345.
39. Snow, A. D., Mar, H., Nochlin, D., Kimata, K., Kato, M., Suzuki, S., Hassell, J., and Wight, T. N. (1988) *Am. J. Pathol. 133*, 456−463.
40. Ghiso, J., Matsubara, E., Koudinov, A., Choi-Miura, N. H., Tomita, M., Wisniewski, T., and Frangione, B. (1993) *Biochem. J. 293* (Part 1), 27−30.
41. Strittmatter, W. J., Weisgraber, K. H., Huang, D. Y., Dong, L. M., Salvesen, G. S., Pericak-Vance, M., Schmechel, D., Saunders, A. M., Goldgaber, D., and Roses, A. D. (1993) *Proc. Natl. Acad. Sci. U.S.A. 90*, 8098−8102.
42. Pepys, M. B., Rademacher, T. W., Amatayakul-Chantler, S., Williams, P., Noble, G. E., Hutchinson, W. L., Hawkins, P. N., Nelson, S. R., Gallimore, J. R., Herbert, J., et al. (1994) *Proc. Natl. Acad. Sci. U.S.A. 91*, 5602−5606.
43. Yasojima, K., Schwab, C., McGeer, E. G., and McGeer, P. L. (1999) *Am. J. Pathol. 154*, 927−936.
44. Biere, A. L., Ostaszewski, B., Stimson, E. R., Hyman, B. T., Maggio, J. E., and Selkoe, D. J. (1996) *J. Biol. Chem. 271*, 32916−32922.
45. Abraham, C. R., Selkoe, D. J., and Potter, H. (1988) *Cell 52*, 487−501.
46. Du, Y., Ni, B., Glinn, M., Dodel, R. C., Bales, K. R., Zhang, Z., Hyslop, P. A., and Paul, S. M. (1997) *J. Neurochem. 69*, 299−305.
47. Ueda, K., Fukushima, H., Masliah, E., Xia, Y., Iwai, A., Yoshimoto, M., Otero, D. A., Kondo, J., Ihara, Y., and Saitoh, T. (1993) *Proc. Natl. Acad. Sci. U.S.A. 90*, 11282−11286.

BI010375C